

# Compressible Sub-Alfvénic MHD turbulence in Low $\beta$ Plasmas

Jungyeon Cho and A. Lazarian

*Astronomy Dept., Univ. of Wisconsin, Madison, WI53706, USA; cho, lazarian@astro.wisc.edu*

(Dated: November 2, 2018)

We present a model for compressible sub-Alfvénic isothermal magnetohydrodynamic (MHD) turbulence in low  $\beta$  plasmas and numerically test it. We separate MHD fluctuations into 3 distinct families - Alfvén, slow, and fast modes. We find that, production of slow and fast modes by Alfvén turbulence is suppressed. As a result, Alfvén modes in compressible regime exhibit scalings and anisotropy similar to those in incompressible regime. Slow modes passively mimic Alfvén modes. However, fast modes show isotropy and a scaling similar to acoustic turbulence.

PACS numbers: 52.35.Bj, 47.65.+a, 52.30.-q 52.35.Ra

## I. INTRODUCTION

Most astrophysical fluids, including stellar winds and the interstellar medium (ISM), are turbulent [1, 7] with an embedded magnetic field that influences almost all of their properties. High interstellar Reynolds numbers ( $Re \equiv L\delta V/\nu > 10^8$ ;  $L$ =the characteristic scale or driving scale of the system,  $\delta V$ =the velocity difference over this scale, and  $\nu$ =viscosity) ensure that. Turbulence spans from km to kpc scales and holds the key to many astrophysical processes (e.g., star formation, fragmentation of molecular clouds, heat and cosmic ray transport, magnetic reconnection). Statistics of turbulence is also essential for the CMB foreground studies [15].

Kolmogorov scalings [13] were the first major advance in the theory of incompressible (non-magnetized) turbulence. Kolmogorov theory predicts an isotropic power law energy spectrum ( $E(k) \propto k^{-5/3}$ ) in wave-vector space  $\mathbf{k}$ .

Attempts to describe magnetic incompressible turbulence statistics were made by Iroshnikov [11] and Kraichnan [14]. Their model of turbulence (IK theory) is isotropic in spite of the presence of the magnetic field and predicts  $k^{-3/2}$  power law energy spectra for both velocity and magnetic field. However, the assumption of isotropic energy distribution in wave-vector space has been criticized by many researchers [21, 22].

An ingenious model very similar in its beauty and simplicity to the Kolmogorov model has been proposed by Goldreich & Sridhar [8] (hereinafter GS95) for incompressible MHD turbulence. It predicts a Kolmogorov-like energy spectra ( $E(k_{\perp}) \propto k_{\perp}^{-5/3}$ ) in terms of wave-vector component  $k_{\perp}$  which is perpendicular to the local direction of magnetic field. The parallel component of the wave-vector  $k_{\parallel} \propto k_{\perp}^{2/3}$  within the model. Numerical simulations [5, 6, 19] support the GS95 model.

In this paper, we study compressible supersonic sub-Alfvénic MHD turbulence in low- $\beta$  plasmas.

## II. THEORETICAL CONSIDERATIONS

While the GS95 model describes incompressible MHD turbulence well, no accepted theory exists for compressible MHD turbulence. Earlier theoretical and numerical efforts [10, 20, 25] addressed effects of compressibility for limited parameter spaces. In (isothermal) plasmas, there are 3 types of MHD waves - Alfvén, slow, and fast waves. Alfvén modes are incompressible while slow and fast modes are compressible. Lithwick & Goldreich [16] conjectured that Alfvén modes follow the GS95 model and slow modes passively follow the same scalings for high  $\beta$  ( $\equiv P_g/P_B \approx 2a^2/V_A^2$ ;  $P_g$ =gas pressure,  $P_B$ =magnetic pressure;  $a$ =sound speed;  $V_A$ =Alfvén speed) regime, which is largely similar to the exactly incompressible regime. They also mentioned that this relation can carry on for low  $\beta$  plasmas.

In the ISM  $\beta$  is frequently less than unity. For instance, it is  $\sim 0.1$  or less for molecular clouds. Therefore, we consider low  $\beta$  regime in this paper. Interstellar turbulence is traditionally thought to be sub-Alfvénic ( $\delta V < V_A$ ), although this is not a universally accepted assumption (see e.g. [3]). If turbulence is super-Alfvénic initially, we expect that eventually magnetic energy should approach the equipartition level [4] and the scales smaller than the energy injection scale should fall in the sub-Alfvénic compressible regime.

Arguments in GS95 are suggestive that the coupling of Alfvén to fast and slow modes will be weak. Consequently, we expect that in this regime the Alfvén cascade should follow the GS95 scaling. Moreover the slow modes are likely to evolve passively (see [16]), so that we expect the GS95 scaling for them as well. However, fast modes are expected to show isotropic distribution as their velocity does not depend on magnetic field direction. To test those theoretical conjectures we use numerical simulations.

### III. NUMERICAL METHOD

To mitigate spurious oscillations near shocks, we combine two essentially non-oscillatory (ENO) schemes. When variables are sufficiently smooth, we use the 3rd-order Weighted ENO scheme [12] without characteristic mode decomposition. When opposite is true, we use the 3rd-order Convex ENO scheme [17]. We use a three-stage Runge-Kutta method for time integration. We solve the ideal MHD equations in a periodic box:

$$\begin{aligned} \partial\rho/\partial t + \nabla \cdot (\rho\mathbf{v}) &= 0, \\ \partial\mathbf{v}/\partial t + \mathbf{v} \cdot \nabla\mathbf{v} + \rho^{-1}\nabla(a^2\rho) - (\nabla \times \mathbf{B}) \times \mathbf{B}/4\pi\rho &= \mathbf{f}, \\ \partial\mathbf{B}/\partial t - \nabla \times (\mathbf{v} \times \mathbf{B}) &= 0, \end{aligned}$$

with  $\nabla \cdot \mathbf{B} = 0$  and an isothermal equation of state. Here  $\mathbf{f}$  is a random large-scale driving force,  $\rho$  is density,  $\mathbf{v}$  is the velocity, and  $\mathbf{B}$  is magnetic field. The rms velocity  $\delta V$  is maintained to be approximately unity, so that  $\mathbf{v}$  can be viewed as the velocity measured in units of the r.m.s. velocity of the system and  $\mathbf{B}/\sqrt{4\pi\rho}$  as the Alfvén speed in the same units. The time  $t$  is in units of the large eddy turnover time ( $\sim L/\delta V$ ) and the length in units of  $L$ , the scale of the energy injection. The magnetic field consists of the uniform background field and a fluctuating field:  $\mathbf{B} = \mathbf{B}_0 + \mathbf{b}$ .

For mode coupling studies (Fig. 1), we use  $144^3$  grid points and we do *not* drive turbulence. We explicitly vary the Alfvén speed of the background field,  $V_A = B_0/\sqrt{4\pi\rho_0}$ , and/or the sound speed. Here  $\rho_0$  is the average density. For scaling studies (Fig. 2), we drive turbulence solenoidally in Fourier space and use  $216^3$  points,  $V_A = 1$ ,  $\rho_0 = 1$ , and  $a = \sqrt{0.1}$ . The average rms velocity in statistically stationary state is  $\delta V \sim 0.7$ . Therefore, the scaling results reported here utilize  $M_s (= \delta V/a) \sim 2.2$ ,  $M_A (= \delta V/V_A) \sim 0.7$ , and  $\beta \sim 0.2$ .

### IV. RESULTS

**Mode coupling of MHD waves.**— We first describe how to separate Alfvén, slow, and fast modes in wave-vector (or, Fourier) space. In general, displacement vectors (hence  $\mathbf{v}_k$ ) of slow waves and fast waves are

$$\hat{\xi}_s \propto k_{\parallel}\hat{\mathbf{k}}_{\parallel} + \frac{1 - \sqrt{D} - \beta/2}{1 + \sqrt{D} + \beta/2} \left[ \frac{k_{\parallel}}{k_{\perp}} \right]^2 k_{\perp}\hat{\mathbf{k}}_{\perp}, \quad (1)$$

$$\hat{\xi}_f \propto \frac{1 - \sqrt{D} + \beta/2}{1 + \sqrt{D} - \beta/2} \left[ \frac{k_{\perp}}{k_{\parallel}} \right]^2 k_{\parallel}\hat{\mathbf{k}}_{\parallel} + k_{\perp}\hat{\mathbf{k}}_{\perp}, \quad (2)$$

where  $D = (1 + \beta/2)^2 - 2\beta\cos^2\theta$  and  $\theta$  is the angle between  $\mathbf{k}$  and  $\mathbf{B}_0$ . In the limit of  $\beta \rightarrow 0$ , the displacement vectors of the slow waves are almost parallel to  $\mathbf{k}_{\parallel}$  ( $\parallel \mathbf{B}_0$ ) and those of fast modes are almost parallel to  $\mathbf{k}_{\perp}$  ( $\perp \mathbf{B}_0$ ). We can obtain slow and fast velocity by projecting velocity component  $\mathbf{v}_k$  into  $\hat{\xi}_s$  and  $\hat{\xi}_f$ , respectively. We can obtain velocity and magnetic field due

to Alfvén modes in the same way as in incompressible case (see [19]):  $\hat{\xi}_A = \hat{\mathbf{k}}_{\parallel} \times \hat{\mathbf{k}}_{\perp}$ . To separate slow and fast magnetic modes, we assume the linearized continuity equation ( $\omega\rho_k = \rho_0\mathbf{k} \cdot \mathbf{v}_k$ ) and the induction equation ( $\omega\mathbf{b}_k = \mathbf{k} \times (\mathbf{B}_0 \times \mathbf{v}_k)$ ) are *statistically* true. From these, we get Fourier components of density and *non-Alfvénic* magnetic field:

$$\begin{aligned} \rho_k &= (\rho_0\Delta v_{k,s}/c_s)\hat{\mathbf{k}} \cdot \hat{\xi}_s + (\rho_0\Delta v_{k,f}/c_f)\hat{\mathbf{k}} \cdot \hat{\xi}_f \\ &\equiv \rho_{k,s} + \rho_{k,f}, \end{aligned} \quad (3)$$

$$\begin{aligned} b_k &= (B_0\Delta v_{k,s}/c_s)|\hat{\mathbf{B}}_0 \times \hat{\xi}_s| + (B_0\Delta v_{k,f}/c_f)|\hat{\mathbf{B}}_0 \times \hat{\xi}_f| \\ &\equiv b_{k,s} + b_{k,f} \end{aligned} \quad (4)$$

$$\begin{aligned} &= \rho_{k,s}(B_0/\rho_0)(|\hat{\mathbf{B}}_0 \times \hat{\xi}_s|/\hat{\mathbf{k}} \cdot \hat{\xi}_s) \\ &+ \rho_{k,f}(B_0/\rho_0)(|\hat{\mathbf{B}}_0 \times \hat{\xi}_f|/\hat{\mathbf{k}} \cdot \hat{\xi}_f), \end{aligned} \quad (5)$$

where  $\Delta v_k \propto v_k^+ - v_k^-$  (superscripts ‘+’ and ‘-’ represent opposite directions of wave propagation) and subscripts ‘s’ and ‘f’ stand for ‘slow’ and ‘fast’ modes, respectively. From equations (3), (4), and (5), we can obtain  $\rho_{k,s}$ ,  $\rho_{k,f}$ ,  $b_{k,s}$ , and  $b_{k,f}$  in Fourier space. We obtain energy spectra (Fig. 2a,c,e) using this projection method done in Fourier space. When we calculate structure functions (Fig. 2b,f) we first obtain the Fourier components using the projection and, then, we obtain the real space values by performing inverse Fourier transform of the projected components. However, we use a different method for the structure function of slow mode velocity (see Fig. 2d).

The dispersion relation of Alfvén modes and those of slow and fast modes in  $\beta \rightarrow 0$  limit are  $\omega = V_A k_{\parallel}$ ,  $\omega = ak_{\parallel}$ , and  $\omega = V_A k$ , respectively. Alfvén modes are not susceptible to collisionless damping. Therefore, we mainly consider transfer of energy from Alfvén modes to the compressible MHD ones (i.e. slow and fast).

To check the strength of the coupling, we first perform a forced supersonic sub-Alfvénic MHD simulation with  $B_0/\sqrt{4\pi\rho_0} = 1$ . Using the same data cube obtained from this simulation, we perform several decaying MHD simulations. We go through the following procedures before we let the turbulence decay. We first remove slow and fast modes in Fourier space and retain only Alfvén modes. We also change the value of  $\mathbf{B}_0$  preserving its original direction. We use the same constant initial density  $\rho_0$  for all simulations. We assign a new constant initial gas pressure  $P_g$  [26]. Note that  $\beta = P_g/(B_0/8\pi)^2$ . After doing all these procedures, we let the turbulence decay. We repeat the above procedures for different values of  $B_0$  and  $P_g$ . Fig. 1a shows time evolution of kinetic energy of a simulation. The solid line represents the kinetic energy of Alfvén modes. It is clear that Alfvén waves do not efficiently generate slow and fast modes. Therefore we expect that Alfvén modes follow the same scaling relation as in incompressible case. Fig. 1b shows that the following relation fits the data well:

$$(\delta V)_f^2/(\delta V)_A^2 \propto (\delta V)_A/B_0, \quad (6)$$

which means the coupling gets weaker as  $B_0$  increases [27]. Note that  $(\delta V)_A$  and  $\rho_0$  are constants. This

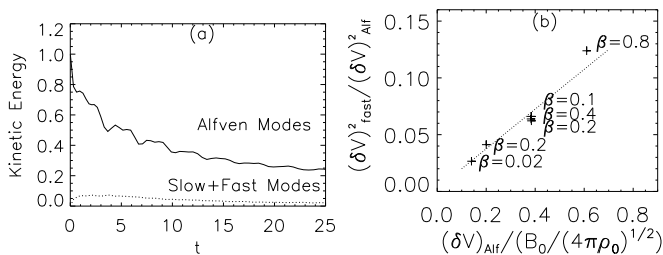


FIG. 1: (a) Decay of Alfvénic turbulence. The generation of fast and slow waves is not efficient. Initially,  $\beta \sim 0.2$  and  $B_0/\sqrt{4\pi\rho_0} = 1$ . (b) The ratio of  $(\delta V)_f^2$  to  $(\delta V)_A^2$ . The ratio is measured at  $t \sim 3$  for all simulations. The ratio strongly depends on  $B_0$ , but only weakly on (initial)  $\beta$ . The initial Mach numbers span 1 – 4.5.

marginal coupling agrees well with a claim in GS95, incompressible simulations [19], and earlier studies where the velocity was decomposed into a compressible component and a solenoidal component [2, 20].

**Alfvén Modes.**— Fig. 2a shows that the spectra of Alfvén waves follow a Kolmogorov spectrum:

$$\text{Alfvén Waves: } E^A(k) \propto k_{\perp}^{-5/3}. \quad (7)$$

In Fig. 2b, we plot the second-order structure function for velocity ( $SF_2(\mathbf{r}) = \langle \mathbf{v}(\mathbf{x} + \mathbf{r}) - \mathbf{v}(\mathbf{x}) \rangle_{\text{avg. over } \mathbf{x}}$ ) obtained in local coordinate systems in which the parallel axis is aligned with the local mean field (see [5, 6, 19]). The  $SF_2$  along the axis perpendicular to the local mean magnetic field follows a scaling compatible with  $r^{2/3}$ . The  $SF_2$  along the axis parallel to the local mean field follows steeper  $r^1$  scaling. The results are compatible with the GS95 model ( $r_{\parallel} \propto r_{\perp}^{2/3}$ , or  $k_{\parallel} \propto k_{\perp}^{2/3}$ ).

**Slow waves.**— The incompressible limit of slow waves is pseudo-Alfvén waves. Goldreich & Sridhar [9] argued that the pseudo-Alfvén waves are slaved to the shear-Alfvén (i.e. ordinary Alfvén) waves, which means that pseudo-Alfvén modes do not cascade energy for themselves (see also [16]). We confirm that similar arguments are applicable to slow waves in low  $\beta$  plasmas. Energy spectra in Fig. 2c are consistent with:

$$\text{Slow Modes: } E^s(k) \propto k_{\perp}^{-5/3}. \quad (8)$$

In Fig. 2d, contours of equal second-order structure function ( $SF_2$ ), representing eddy shapes, show scale-dependent isotropy: smaller eddies are more elongated. The results are compatible with the GS95 model ( $k_{\parallel} \propto$

$k_{\perp}^{2/3}$ , or  $r_{\parallel} \propto r_{\perp}^{2/3}$ , where  $r_{\parallel}$  and  $r_{\perp}$  are the semi-major axis and semi-minor axis of eddies, respectively [5]).

From the linearized continuity equation and the induction equation, we can show that density fluctuations are dominated by slow waves and only a small amount of magnetic field is produced by the slow waves in low  $\beta$  plasmas:  $(\delta\rho/\rho)_s = (\delta V)_s/a \sim M_s$ , and  $(\delta B)_s \rightarrow 0$ , as  $\beta \rightarrow 0$ . Here  $M_s$  is the sonic Mach number. When  $M_s \gg 1$ , the above relation for density fluctuation may not give a good approximation.

**Fast waves.**— Fig. 2f shows fast modes are isotropic. The resonance conditions for the interacting fast waves are  $\omega_1 + \omega_2 = \omega_3$  and  $\mathbf{k}_1 + \mathbf{k}_2 = \mathbf{k}_3$ . Since  $\omega \propto k$  for the fast modes, the resonance conditions can be met only when all three  $\mathbf{k}$  vectors are collinear. This means that the direction of energy cascade is *radial* in Fourier space. This is very similar to acoustic turbulence, turbulence caused by interacting sound waves [18, 23, 24]. Zakharov & Sagdeev [24] found  $E(k) \propto k^{-3/2}$ . However, there is debate about the exact scaling of acoustic turbulence. Here we cautiously claim that our numerical results are compatible with the Zakharov & Sagdeev scaling:

$$\text{Fast Modes: } E^f(k) \sim k^{-3/2}. \quad (9)$$

Non-Alfvénic magnetic field perturbations are mostly affected by fast modes when  $\beta$  is small:  $(\delta B)_f \sim (\delta V)_f$ , which is larger than  $(\delta B)_s \approx 0$ .

Turbulent cascade of fast modes is expected to be slow and in the absence of collisionless damping they are expected to persist in turbulent media over longer timespans than Alfvén or slow modes. This effect is difficult to observe within numerical simulations where  $\Delta B \sim B_0$ .

## V. CONCLUSION

We found that, in the isothermal supersonic sub-Alfvénic low- $\beta$  plasmas, the following scalings are valid:

1. Alfvén:  $E^A(k) \propto k^{-5/3}$ ,  $k_{\parallel} \propto k_{\perp}^{2/3}$ ,
2. Slow:  $E^s(k) \propto k^{-5/3}$ ,  $k_{\parallel} \propto k_{\perp}^{2/3}$ ,
3. Fast:  $E^f(k) \propto k^{-3/2}$ , isotropic energy spectra.

**Acknowledgments** We thank Peter Goldreich for many useful suggestions, his encouragement, and refereeing this paper. We acknowledge the support of NSF Grant AST-0125544. This work was partially supported by NCSA under AST010011N and utilized the NCSA Origin2000.

[1] J. W. Armstrong, B. J. Rickett, & S. R. Spangler, *Astrophys. J.* **443**, 209 (1995)  
 [2] S. Boldyrev, A. Nordlund, & P. Padoan, *astro-ph/0111345* (2001)

[3] S. Boldyrev, *Astrophys. J.* **569**, 841 (2002)  
 [4] J. Cho & E. T. Vishniac, *Astrophys. J.* **538**, 217 (2000)  
 [5] J. Cho & E. T. Vishniac, *Astrophys. J.* **539**, 273 (2000)  
 [6] J. Cho, A. Lazarian, & E. T. Vishniac, *Astrophys. J.*

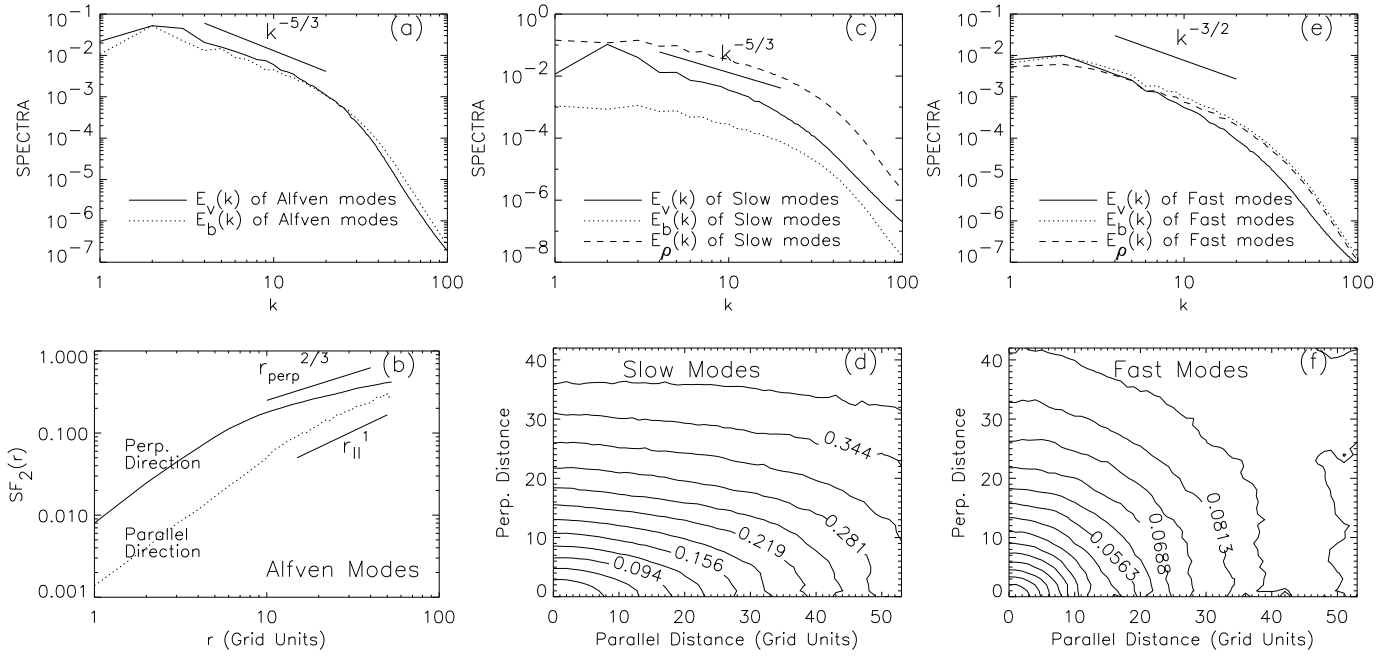


FIG. 2: Scalings relations. Results from driven turbulence with  $M_s \sim 2.2$ ,  $M_A \sim 0.7$ ,  $\beta \sim 0.2$ , and  $216^3$  grid points. (a) Spectra of Alfvén modes follow a Kolmogorov-like power law. (b) The second-order structure function ( $SF_2$ ) for velocity of Alfvén modes shows anisotropy similar to the GS95 ( $r_{\parallel} \propto r_{\perp}^{2/3}$  or  $k_{\parallel} \propto k_{\perp}^{2/3}$ ). The structure functions are measured in directions perpendicular or parallel to the local mean magnetic field in real space. We obtain real-space velocity and magnetic fields by inverse Fourier transform of the projected fields. (c) Spectra of slow modes also follow a Kolmogorov-like power law. (d) Slow mode velocity shows anisotropy similar to the GS95. We obtain contours of equal  $SF_2$  directly in real space without going through the projection method, assuming slow mode velocity is nearly parallel to local mean magnetic field in low  $\beta$  plasmas. (e) Spectra of fast modes are compatible with the IK spectrum. (f) The magnetic  $SF_2$  of fast modes shows isotropy. We obtain real-space magnetic field by inverse Fourier transform of the projected fast magnetic field. Fast mode velocity also shows isotropy.

- 564, 291 (2002)
- [7] J. Cho, A. Lazarian, & E. T. Vishniac, in *Simulations of magnetohydrodynamic turbulence in astrophysics*, eds. by T. Passot & E. Falgarone (Springer Lecture Notes in Physics; 2002), submitted
- [8] P. Goldreich & H. Sridhar, *Astrophys. J.* **438**, 763 (1995) (GS95)
- [9] P. Goldreich & H. Sridhar, *Astrophys. J.* **485**, 680 (1997)
- [10] J. C. Higdon, *Astrophys. J.* **285**, 109 (1984)
- [11] P. Iroshnikov, *Astron. Zh.* **40**, 742 (1963) (English: *Sov. Astron.* **7**, 566 (1964))
- [12] G. Jiang & C. Wu, *J. Comp. Phys.* **150**, 561 (1999)
- [13] A. Kolmogorov, *Dokl. Akad. Nauk SSSR* **31**, 538 (1941)
- [14] R. Kraichnan, *Phys. Fluids* **8**, 1385 (1965)
- [15] A. Lazarian & S. Prunet, in *Astrophysical Polarized Backgrounds*, eds. by S. Cecchini et al. (AIP Conf. Proc. Vol. 609, 2002) p32 (astro-ph/0111214)
- [16] Y. Lithwick & P. Goldreich, *Astrophys. J.* **562**, 279 (2001)
- [17] X. Liu & S. Osher, *J. Comp. Phys.* **141**, 1 (1998)
- [18] V. S. L'vov, Y. V. L'vov, & A. Pomyalov, *Phys. Rev. E*, **61**, 2586, (2000)
- [19] J. Maron & P. Goldreich, *Astrophys. J.* **554**, 1175 (2001)
- [20] W. M. Matthaeus, S. Ghosh, S. Oughton, & D. A. Roberts, *J. Geophys. Res.* **101**, 7619 (1996)
- [21] D. C. Montgomery, *Physica Scripta* **T2/1**, 83 (1982)
- [22] J. V. Shebalin, W. H. Matthaeus, & D. C. Montgomery, *J. Plasma Phys.* **29**, 525 (1983)
- [23] V. E. Zakharov, *Sov. Phys. JETP*, **24**, 455 (1967)
- [24] V. E. Zakharov & A. Sagdeev, *Sov. Phys. Dokl.* **15**, 439 (1970)
- [25] G. P. Zank & W. H. Matthaeus, *Phys. Fluids A* **5**(1), 257 (1993)
- [26] The changes of both  $B_0$  and  $P_g$  preserve the Alfvén character of perturbations. In Fourier space, the mean magnetic field ( $\mathbf{B}_0$ ) is the amplitude of  $\mathbf{k} = \mathbf{0}$  component. Alfvén components in Fourier space are for  $\mathbf{k} \neq \mathbf{0}$  and their directions are parallel/anti-parallel to  $\hat{\xi}_A (= \hat{\mathbf{B}}_0 \times \hat{\mathbf{k}}_{\perp})$ . The direction of  $\hat{\xi}_A$  does not depend on the magnitude of  $B_0$  or  $P_g$ .
- [27] The wandering of large scale (i.e. energy injection scale) magnetic field may interfere with our projection method. However, we first note that this effect is no larger than  $\sim (\delta V)_A^2 / B_0^2$  [5, 19]. Second, the generated fast modes show isotropy similar to Fig. 2f. Alfvén modes are anisotropic. Therefore, it is not likely that the measured isotropic mode is a numerical artifact.